Cambridge Environmental Research Consultants Ltd

Development of boundary layer profiles for offshore dispersion modelling

Final Report

Prepared for
Department of Trade and Industry

1 April 2004

CERC

Report Information

CERC Job Number:	FM581
Job Title:	Development of boundary layer profiles for offshore dispersion modelling
Prepared for:	Department of Trade and Industry
Report Status:	Final
Report Reference:	FM581/R3/04
Issue Date:	1 April 2004
Author(s):	Stephanie Dyster, David Carruthers
Reviewer(s):	David Carruthers

Issue	Date	Comments
1	3 Feb 2004	First draft
2	1 Apr 2004	Final

Main File(s):	FM581_R3_01Apr04.doc
Figures and Tables	Model Run Reference(s)
	See runs summary spreadsheets

Contents

1. EXECUTIVE SUMMARY

The Department of Trade and Industry (DTI) commissioned Cambridge Environmental Research Consultants Limited (CERC) to investigate how the atmospheric boundary layer differs over the sea from that over the land, and the implications of these differences for atmospheric dispersion modelling of releases from offshore sources. Specifically, CERC were asked to complete the following tasks:

a) Review available meteorological data offshore, and purchase/obtain data appropriate for the current study.

b) Carry out a literature review on previous work done in this area.

c) Carry out studies to test the sensitivity of currently available model boundary layer profiles to changes in model input parameters.

d) Develop new schemes for representing the marine atmospheric boundary layer in practical dispersion modelling.

In this study, standard meteorological data at sites in the North Sea are found to be available for purchase from a limited number of sources. Useful sources of sea surface temperature data and wave data are also identified.

Previous work on the parameterisation of the vertical wind profile and sensible and latent heat fluxes over the sea is summarised. The surface roughness, wind and wave parameters are all co-dependent. Methods of parameterising the surface roughness as a function of wind speed or of wave parameters are presented. Methods of parameterising the sensible and latent heat fluxes as functions of the air-sea temperature difference and the vertical humidity profile respectively are also described.

A number of current and proposed methods of representing the offshore boundary layer are tested using the practical air dispersion model ADMS. It is seen that allowing the surface roughness to vary with the wind speed tends to increase predicted levels of turbulence. This decreases ground level concentrations for elevated passive releases by about 10-15%, whilst increasing ground level concentrations for elevated buoyant releases by about the same amount. It is found that the choice of heat flux scheme has a larger difference on dispersion modelling results than the choice of surface roughness parameterisation, changing calculated concentration results for the sources modelled by up to 80%. When a marine heat flux scheme is used, long term mean and low percentile concentrations are higher than those obtained when a land heat flux scheme is used, but maximum (high percentile) concentrations are lower.

Modelled results obtained using surface roughness varying with wind speed and the new marine heat flux schemes are compared with observed data from a site in the Baltic Sea. Trends are well predicted, with a high correlation between modelled and observed data. However, absolute values suggest that the optimal values of the Charnock parameter in such a coastal area is higher than values that would be routinely used for the open sea.

Based on these studies it is recommended that the following is a satisfactory parameterisation of the marine boundary layer for offshore dispersion studies when the immediate fetch is over the sea:

- Surface roughness and wind profile parameterised using Equation 4.3 (page 9). For typical coastal waters, the Charnock parameter α_{Ch} should take the value 0.08.

- Surface layer heat fluxes parameterised using Equations 4.7 and 4.11 (page 11).

Note that when using this scheme, the surface roughness (z_0), friction velocity (u_*) and Monin-Obukhov length (L_{MO}) need to be calculated by iteration.

If the site under consideration is directly adjacent to land and the wind is offshore, the usual land-based parameterisation should be utilised.

It is recommended that further work be undertaken to investigate typical spatial and temporal variation of α_{Ch}, for example using the data that will soon be available from the FINO project. It would then be possible to recommend values of α_{Ch} for different types of marine location.

2. INTRODUCTION

The Department of Trade and Industry (DTI) commissioned Cambridge Environmental Research Consultants Limited (CERC) to investigate how the atmospheric boundary layer differs over the sea from that over the land, and the implications of these differences for atmospheric dispersion modelling of releases from offshore sources. Specifically, CERC were asked to complete the following tasks:

e) Review available meteorological data offshore, and purchase/obtain data appropriate for the current study.

f) Carry out a literature review on previous work done in this area.

g) Carry out studies to test the sensitivity of currently available model boundary layer profiles to changes in model input parameters.

h) Develop new schemes for representing the marine atmospheric boundary layer in practical dispersion modelling.

The availability of offshore meteorological data (Task (a)) is discussed in Section 3. A literature review of previous work on parameterisations of the marine boundary layer (Task (b)) is presented in Section 4. In Section 5 a number of proposed methods of modelling the marine boundary layer within an atmospheric dispersion model, ADMS, are presented (Tasks (c) and (d)). A sensitivity study is carried out, and comparisons with observed data are presented. In Section 6 the results of the study are discussed and some recommendations for practical dispersion modelling offshore are made. Finally, Appendix A gives an overview of the ADMS air quality model used in the study.

3. AVAILABILITY OF OFFSHORE DATA

Meteorological data are key input data for dispersion modelling calculations. As part of the current study, CERC were therefore asked to identify bodies collecting offshore met data in the North Sea, and to investigate the availability and associated costs of historical data.

A typical dispersion study requires the following routinely observed met data:

- Wind speed and direction
- Air temperature
- Cloud cover
- Relative (or specific) humidity.

Sources of offshore measurements of these data are discussed in Section 3.1.

For the purposes of the current study, more detailed met data will be of use in validating proposed parameterisations of the marine boundary layer. Ideally, these data would include measurements of wind, temperature, humidity, turbulence and heat fluxes at various heights above sea level. These data would typically be collected during research projects. The availability of such data is discussed in Section 3.2.

For studies of dispersion over the sea, oceanographic data are also of importance. As discussed in Section 4, the marine boundary layer is strongly influenced by sea surface temperature. In the current study it will also be of interest to investigate the relationship between waves and the atmospheric boundary layer – for this purpose wave lengthscales (such as wave height) and timescales (such as wave period) are required. Sources of these data are described in Section 3.3.

Contact details for all the useful sources of data identified are summarised in Table 3.1 at the end of this Section.

3.1 Routine meteorological observations

The main providers of routinely observed meteorological parameters are national met services. For North Sea data, the Dutch met service **KNMI** is particularly useful. Hourly observations of all the standard parameters are available from 11 coastal sites and 7 North Sea platforms, at a basic price of 0.032 EURO per piece. Details, including a map showing measurement locations, are available from the website. The **UK Met Office** sells hourly observations of all the standard parameters in a format suitable for immediate input into the ADMS dispersion model, at various land-based sites in the UK, some of which are coastal, at a price of £440 for one year of all parameters from one site (with economies of scale for multiple years). Forecast model data over the sea are also available. More details are available from the website.

The **Press Association (PA) Weather Centre** is able to provide data from a number of observation stations in the North Sea, most of which are oil rigs. Most of the standard parameters are available, although cloud cover measurements are fairly sparse. The cost

of the data is £150 for one year of data from one site (with economies of scale for multiple sites).

The DTI have contacted all the major North Sea oil installation operators on behalf of CERC to enquire whether they are able to provide data. The response has been fairly limited, and is summarised below.

- **Shell** measure wind and temperature at over 20 platforms, at some of which wave, cloud and visibility data are also measured. Data can be supplied if not used for commercial gain.
- **Talisman Energy** take measurements at various platforms, the most useful of which are
    - Tartan Platform (situated in the mid North Sea), which records wind, temperature and relative humidity.
    - Beatrice Platform (situated in the Moray Firth, 24km from the coast), which records wind temperature and humidity (instantaneous, 2 minute and 10 minute averages).
- **Hydrocarbons Resources Ltd**. (HRL) run an offshore UK Met Office weather station in Morecambe Bay, from which data should be available to purchase from the Met Office, and a wave monitoring station, from which data are available from HRL.

3.2 Detailed meteorological observations

The following sources of data have been identified as potentially the most useful:

- **German Wind Energy Institute (DEWI)**
  The German government is currently funding a project (FINO) to set up offshore measurement platforms in the North Sea and Baltic Sea, with the aim of expanding knowledge of the offshore environment for the purposes of wind farm planning. (See www.fino-offshore.com for further information.) The German Wind Energy Institute (DEWI) is responsible for setting up the platforms and carrying out measurements. Data from the first platform, 45km north of the island of Borkum in the North Sea, are due to be available shortly. Wind, turbulence, temperature and humidity measurements will be taken up to 101m above sea level. Oceanographic measurements will include wave height and sea surface temperature. Data will be freely available via a website.

- **ELSAM**
  The Danish power company ELSAM collect all the required meteorological and oceanographic data at a mast at Horns Rev, a wind farm located 14-20km west of the west Danish coast (www.hornsrev.dk). Measurements began 3 years ago. Meteorological measurements are made at four heights, up to 64m above sea level. The cost and availability of data are currently under investigation.

- **RISØ**
  The Danish research institution RISØ were involved in measurements of wind, temperature and humidity, heat fluxes and turbulence in the Baltic Sea over a period of about 10 days in Autumn 1998. Measurements were made 10m above sea level, close to the small islands of Christiansø, 20km to the north-east of the

larger island of Bornholm. Limited measurements of sea surface temperature were also taken. The measurements were part of the larger project PEP-in-BALTEX (Pilot study on evaporation and precipitation over the Baltic Sea), supported by the EU. The experiments are described in various published scientific papers (for example [7]), and discussed further in Section 5.3.

3.3 Oceanographic data

The German organisation **Bundesamt fur Seeschifffahrt und Hydrographie** (BSH) was found to be a good source of sea surface temperature data. Monthly and weekly average maps of sea surface temperature in the North Sea are available, from 1995 to the present. Since the sea surface temperature varies slowly, these data should be sufficiently accurate for dispersion modelling.

Maps of summer average temperatures are available from the UK **Centre for Environment Fisheries and Aquaculture Science** (CEFAS), who are also able to provide limited historical wave height data from a few UK coastal sites.

Detailed historical wave data from 1979 to the present, including wave height and period, at a number of sites off the Dutch coast, are available to download from the website of the **Dutch National Institute for Coastal and Marine Management** (RIKZ). The data also include wind measurements.

Table 3.1 Contact details for meteorological and oceanographic data

Routine meteorological data	
KNMI	Summary of available data in English: http://www.knmi.nl/wrma/WRMA_hist_weather_data_neth.htm
UK Met Office	Observed data: http://www.metoffice.com/environment/serv10.html Model data: http://www.metoffice.com/environment/serv7.html
PA Weather Centre	Contact Andy Giles (Andy.Giles@pa.press.net)
Shell	Contact Paul Chatwin (Paul.Chatwin@Shell.com)
Talisman	Contact Jan Rusin (jrusin@talisman.co.uk)
Hydrocarbon Resources Ltd.	Contact Brian Helliwell (HELLIWELL.BK@hrl.co.uk)
Detailed meteorological data	
DEWI	www.fino-offshore.com
ELSAM	www.hornsrev.dk
RISØ	Please see References
Oceanographic data	
BSH	Sea surface temperature: http://www.bsh.de/en/Marine%20data/Observations/Sea%20surface%20temperatures/anom.jsp#SSTM
CEFAS	Summer sea surface temperature: http://www.cefas.co.uk/fishinfo/surface_temperature.htm#top Wave data: http://www.cefas.co.uk/wavenet/default.htm
RIKZ	Wave data: http://www.golfklimaat.nl/engels/index.html (click 'generate wave climate' then 'data.')

4. REVIEW OF PREVIOUS WORK

For dispersion modelling purposes, the differences between the vertical wind profile and stability of the atmosphere over the sea and those over land are of interest. The basic processes of importance in the marine boundary layer are the same as those over the land – processes within the boundary layer are driven by the geostrophic wind and conditions above the boundary layer, and are affected by surface roughness and heat flux effects. However, there are some fundamental differences between the surface roughness and heat fluxes over the sea and those over the land. The current literature in this field has been investigated – a summary is given below.

4.1 Surface roughness and vertical wind profile

The vertical wind profile can be expressed as a function of the surface roughness, z_0 (m), and the friction velocity, u_* (m/s). Garratt [1] notes that if marine values of these parameters are used, then the same vertical profile functions can be used over the sea as over the land.

Over the sea, the surface roughness will depend on the size and shape of the waves, which in turn depends on the wind speed. Hence the values of z_0 and u_*, and the wave parameters, are co-dependent. Various suggested parameterisations for z_0 over the sea are summarised below.

In light winds z_0 can be parameterised as

$$z_0 = \frac{A\nu}{u_*} \qquad \text{(Eqn 4.1)}$$

where ν (= 1.45×10^{-5} m^2/s) is the kinematic viscosity of air, and Hinze [2] suggests $A \approx 0.11$. In rough seas, the following parameterisation is suggested by Charnock [3]:

$$z_0 = \frac{\alpha_{Ch} u_*^{\,2}}{g} \qquad \text{(Eqn 4.2)}$$

where g is the acceleration due to gravity (= $9.81 m/s^2$) and α_{Ch} is the Charnock parameter. Garratt [1] recommends that observations suggest using a value of α_{Ch} in the range 0.014 to 0.0185, noting however that a value of 0.032 has been commonly used in numerical models of the atmosphere. The transition from 'light winds' to 'rough seas' occurs at a 10m wind speed of around 5.5m/s.

From a practical modelling perspective, the parameterisation used by ECMWF (the European Centre for Medium-Range Weather Forecasting) for z_0 combines Equations 4.1 and 4.2 as follows ([4]):

$$z_0 = \alpha_m \frac{\nu}{u_*} + \alpha_{Ch} \cdot \frac{u_*^2}{g} \qquad \text{(Eqn 4.3)}$$

where $\alpha_m = 0.11$ and $\alpha_{Ch} = 0.018$. Under this scheme, z_0 takes a minimum value when $u_* = u_{*\,CRIT}$, where $u_{*\,CRIT} = \left(\frac{\alpha_m \nu\, g}{2\alpha_{Ch}} \right)^{1/3}$. Below this value, z_0 increases as u_* decreases, and above this value, z_0 increases with u_*.

It should be noted that whilst this approach and the parameter values used are appropriate in the open sea where the wind has been blowing over the sea for a considerable distance (i.e. there is a long fetch), modifications may be required in other situations. For example, the appropriate value of α_{Ch} will vary, and is expected to be higher near land.

An alternative method is to parameterise z_0 using wave data. Taylor and Yelland [5] summarise previous work in this field where z_0 is expressed as a function of the wave slope or the wave 'age', and suggest the following parameterisation:

$$\frac{z_0}{H_s} = 1200 \left(\frac{H_s}{L_p} \right)^{4.5} \qquad \text{(Eqn 4.4)}$$

where H_s (m) is the significant wave height (defined as the average height of the highest third of the waves) and L_p (m) is the wavelength of the waves at the peak of the wave spectrum (so H_s/L_p is a measure of the wave slope). Typically, where wave measurements are taken, the wave height H_s and period T_p are recorded. The wavelength L_p can be calculated from T_p from standard linear wave theory, by applying a 'deep water' approximation, in which it is assumed that the depth of the water is much greater than the wavelength of the waves ([13]). This yields the following equation:

$$L_p = \frac{g T_p^{\,2}}{2\pi} \qquad \text{(Eqn 4.5)}$$

The parameterisation defined by Equation 4.4 is found to fit many of the available datasets well, although it is less successful for short fetch. It is noted, however, that there may be some difficulty in defining H_s and L_p over the open ocean where waves are created by swell as well as wind.

4.2 Heat fluxes and stability

The temperature of the sea varies only very slowly with incident solar radiation. This is because the sea has a higher specific heat capacity than land, the radiation is absorbed over the first few metres of the depth of the sea rather than just at the surface and there is vertical mixing within the sea. Also, a larger proportion of the incident radiation is used in evaporation, as there is more moisture available. These effects reduce the ratio of the surface sensible heat flux to the latent heat flux, and will tend to cause stability conditions to be more neutral over the sea than over the land (Garratt [1]). This in turn limits the growth of the atmospheric boundary layer over the sea during the day. However, the fact that the sea is a very large source of energy may offset this effect and cause large heat fluxes when cool air is advected over a warmer sea (for example if the land is cooler than the sea and there is an offshore wind).

Panofsky and Dutton [9] parameterise the surface sensible and latent heat fluxes over water by defining separate 'surface roughnesses' for sensible heat (z_{0H}) and moisture (z_{0q}), given by

$$z_{0_H} = \alpha_H \frac{v}{u_*}$$
$$z_{0_q} = \alpha_q \frac{v}{u_*} \qquad \text{(Eqn 4.6)}$$

This approach is adopted by ECMWF [4], with α_H = 0.4 and α_q = 0.62. The surface sensible heat flux $F_{\theta 0}$ is then given by

$$F_{\theta_0} = \frac{-c_p \rho \kappa^2 (\theta(z) - \theta_0) u(z)}{\left[\ln\left(\frac{z+z_{0H}}{z_{0H}}\right) - \psi_H\left(\frac{z+z_{0H}}{L_{MO}}\right)\right]\left[\ln\left(\frac{z+z_0}{z_0}\right) - \psi\left(\frac{z+z_0}{L_{MO}}\right)\right]} \qquad \text{(Eqn 4.7)}$$

([9]) where c_p is the specific heat capacity of air (J/kg/K), ρ is the density of air (kg/m^3), κ is von Karman's constant (= 0.4), θ is potential temperature (K), and θ_0 is the potential temperature corresponding to the temperature of the sea surface. For stable and neutral conditions, ($1/L_{MO} \geq 0$) $\psi_H = \psi$ (as defined in the ADMS Technical Specification [8]), and for convective conditions (the Monin Obukhov length $1/L_{MO} < 0$) ψ_H is given by

$$\psi_H = \ln\left[\frac{(1+y)^2}{(1+y_{surface})^2}\right] \qquad \text{(Eqn 4.8)}$$

where

$$y = \left[1 - 16\left(\frac{z+z_{0_H}}{L_{MO}}\right)\right]^{1/2} \qquad \text{(Eqn 4.9)}$$

$$y_{surface} = \left[1 - 16\left(\frac{z_{0_H}}{L_{MO}}\right)\right]^{1/2} \qquad \text{(Eqn 4.10)}$$

The latent heat flux λE is given similarly by

$$\lambda E = \frac{-\lambda \rho \kappa (q(z) - q_{sat\,0}) u(z)}{\left[\ln\left(\frac{z+z_{0q}}{z_{0q}}\right) - \psi_q\left(\frac{z+z_{0q}}{L_{MO}}\right)\right]\left[\ln\left(\frac{z+z_0}{z_0}\right) - \psi\left(\frac{z+z_0}{L_{MO}}\right)\right]} \qquad \text{(Eqn 4.11)}$$

([9]) where λ is the specific latent heat of vapourisation of water (J/kg), q is the specific humidity, q_{sat0} is the saturation specific humidity at the sea surface, and $\psi_q = \psi_H$.

Again it should be noted that whilst such parameterisations may be used over the open ocean, nearby land can have a significant effect on the boundary layer structure [7].

Mesoscale effects of land-sea transitions including coastal jets are discussed in [11], but are not considered further in this report.

5. APPLICATION TO OFFSHORE MODELLING

In the current study, various methods of representing the marine boundary layer in dispersion modelling have been investigated, with regard to the effect on

- the predicted boundary layer characteristics
- the resulting dispersion of pollution from typical sources.

This has been carried out using CERC's air dispersion model ADMS, which is described in Appendix A. The various representations are described in Section 5.1. In Section 5.2, a sensitivity study comparing a number of the different representations is described. Section 5.3 describes a comparison of one particular representation with observed data. In Section 5.4 the sensitivity study is revisited in the light of the comparison with observed data, and extended to include a representation dependent on wave data.

5.1 Representing the marine boundary layer

The following methods of representing the marine boundary layer have been investigated.

i) Constant surface roughness typical of the sea
ii) Constant surface roughness typical of the sea, neutral boundary layer
iii) Adjusted ratio between the surface sensible and latent heat fluxes
iv) Surface roughness dependent on wind speed, neutral boundary layer
v) Surface roughness dependent on wind speed, marine heat flux algorithms
vi) Surface roughness dependent on wave slope, marine heat flux algorithms

These methods are described in more detail below.

i) Constant surface roughness typical of the sea

Here the velocity profile and heat fluxes were calculated using algorithms developed for use over the land, i.e. those in the standard version of ADMS. The reader is referred to the ADMS Technical Specification ([8]) for details. The constant surface roughness used was a typical value for the sea (on the order of 10^{-4}m). This case provides a useful base case scenario against which to compare more sophisticated approaches.

ii) Constant surface roughness typical of the sea, neutral boundary layer

Here the velocity profile was calculated using algorithms developed for use over the land, i.e. those in the standard version of ADMS, but neutral conditions were assumed (i.e. zero heat fluxes). The constant surface roughness used was a typical value for the sea (on the order of 10^{-4}m). This case provides a useful base case scenario against which to compare scheme (iv) below.

iii) Adjusted ratio between the surface sensible and latent heat fluxes

As noted in Section 4.2, the ratio of the surface sensible heat flux to the latent heat flux (the Bowen ratio) over the sea differs from that over the land, due to the increased moisture availability, among other effects. Although the Bowen ratio cannot be directly input to ADMS, the Priestly-Taylor parameter, which can be derived from the Bowen ratio and the air

temperature, can be input. The relationship between the Bowen ratio and Priestly-Taylor parameter is described in [8]. In options (i) and (ii) above, a value of 1 was used for the Priestly-Taylor parameter. This value is appropriate for moist land conditions. For option (iii), the Priestly-Taylor parameter was calculated from the air temperature and the Bowen ratio, assuming a typical marine value of 0.1 for the Bowen ratio ([10]).

iv) Surface roughness dependent on wind speed, neutral boundary layer

Here the surface roughness and friction velocity were assumed to be co-dependent as specified in Equation 4.3, with $\alpha_m = 0.11$ and $\alpha_{Ch} = 0.018$. This equation and the equations specifying the wind profile (described in the ADMS Technical Specification [8]) were then solved by iteration. Conditions were assumed to be neutral, that is, the sensible and latent heat fluxes were assumed to be zero. This has the advantage that the only meteorological input data required are wind measurements. Modifications were made to ADMS to carry out the calculation of z_0 and u_* from the input wind data.

v) Surface roughness dependent on wind speed, marine heat flux algorithms

Again the surface roughness and friction velocity were assumed to be co-dependent as in (iv) above. In addition, heat fluxes were calculated using Equations 4.6 – 4.11, with $\alpha_H = 0.4$ and $\alpha_q = 0.62$. Again the equations were solved by iteration, within the ADMS model. As well as wind measurements, these calculations require air and sea surface temperature and humidity data as input.

vi) Surface roughness dependent on wave slope, marine heat flux algorithms

Here the surface roughness was calculated from the wave slope, using Equation 4.4. The values of surface roughness were calculated prior to running ADMS, then input to the model to obtain the friction velocity. As in scheme (v) above, heat fluxes were then calculated using Equations 4.5 – 4.10, with $\alpha_H = 0.4$ and $\alpha_q = 0.62$, requiring air and sea surface temperature and humidity data to be input.

5.2 Sensitivity to marine parameterisations

In this section a sensitivity study is presented, comparing the first five marine boundary layer parameterisations described in Section 5.1. (Scheme (vi) is omitted here, as it requires wave measurements, which are less commonly available than wind measurements. However, for further discussion of scheme (vi), see Section 5.4.) The input meteorological data are described in Section 5.2.1, and the typical source parameters used to assess the effect on dispersion are described in Section 5.2.2. Section 5.2.3 describes the effect of each parameterisation on the boundary layer structure, and Section 5.2.4 describes the corresponding effect on dispersion.

5.2.1 Meteorological data

Data for the year 2000 from the Sean Papa oil platform in the North Sea were used. These data were supplied to CERC by Shell UK Exploration and Production (Shell) in Aberdeen for a previous project carried out for the DTI. The platform is located at latitude 53° 11' 20.945" north and longitude 2° 51' 41.729" east.

Dry bulb temperature (°C) was recorded every 10 minutes at 35m above sea level, and these data were averaged to give hourly values for the year.

Wind data were recorded every hour on the hour at a height of 70m above sea level (asl). Wind speed values (m/s) had been corrected to 10m asl using a factor of 0.7955, so this factor was used to recalculate the observed wind speed at 70m asl.

The wave height and period were also recorded every hour.

The data provided by Shell were supplemented by cloud cover and relative humidity data measured at the UK Met Office site at Hemsby, on the North Sea coast, and by monthly average sea surface temperatures at Sean Papa estimated from the maps available from BSH (see Table 3.1).

As a large proportion of the relative humidity measurements for the first six months of the year were missing, only the data for July – December 2000 were used in the current study. The data for this six-month period are summarised in Table 5.1. Note that the average sea surface temperature is slightly higher than the average air temperature – as is to be expected in the second half of the year, the sea is typically slightly warmer than the air. The monthly average sea surface and air temperatures are illustrated in Figure 5.1.

Table 5.1 Summary of input met. data

Parameter	*Minimum*	*Maximum*	*Mean*
Wind speed at 70m (m/s)	0.0*	31.4	9.2
Air temperature at 35m (°C)	0.9	22.5	13.0
Sea surface temperature (°C)	8.3	16.5	13.2
Relative humidity (%)	51	100	81

*Note that no calculations were carried out for wind speeds which were less than 0.75m/s when adjusted to10m

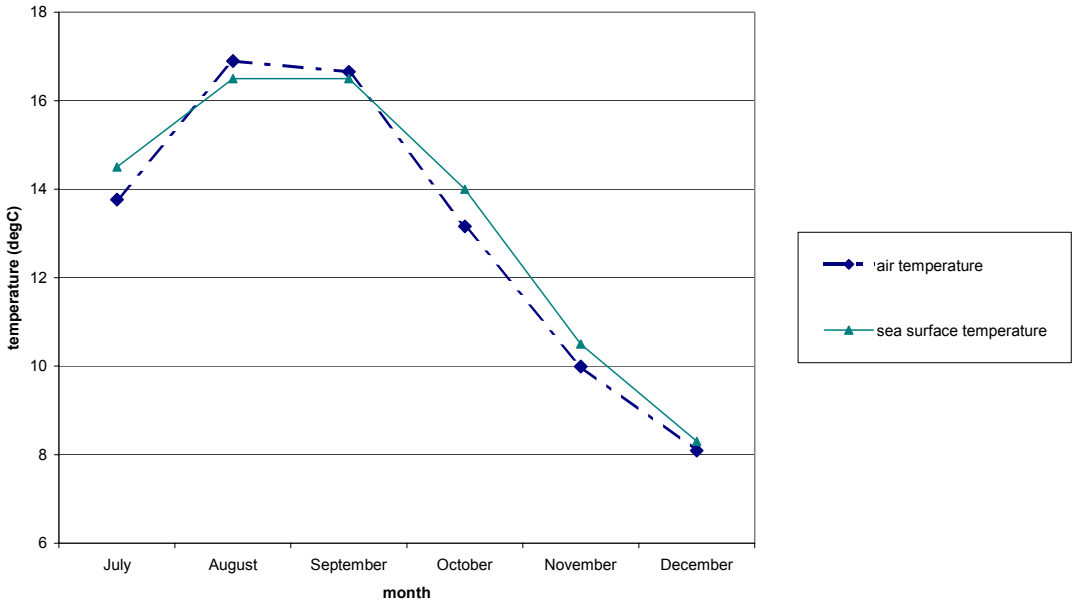

Figure 5.1 Monthly average air and sea surface temperatures at Sean Papa, year 2000

5.2.2 Source data

Two types of point source were modelled. Firstly a series of releases at different heights with no buoyancy or upward momentum were considered, to gain an understanding of the basic effects of the boundary layer structure on dispersion. Secondly a buoyant release such as would typically occur at an offshore oil installation was modelled. The source parameters are listed in Table 5.2. In all cases a standard release rate of 1g/s was assumed.

Table 5.2 Source parameters

Description	*Height (m)*	*Diameter (m)*	*Exit velocity (m/s)*	*Temperature (°C)*
Short passive	5	1	0	(ambient)
Medium passive	30	1	0	(ambient)
High passive	100	1	0	(ambient)
Typical buoyant	35	1.9	6.28	490

5.2.3 Effect on boundary layer structure

The values of z_0, u_* and heat fluxes predicted using the five different parameterisations described in Section 5.1 are summarised in Tables 5.3 to 5.6.

Table 5.3 Predicted values of z_0 (m)

Scheme	*Minimum*	*Maximum*	*Mean*
(i) Constant z_0, land Bowen ratio	2.33E-04*	2.33E-04*	2.33E-04*
(ii) Constant z_0, land Bowen ratio, neutral	2.43E-04†	2.43E-04†	2.43E-04†
(iii) Constant z_0, marine Bowen ratio	2.33E-04*	2.33E-04*	2.33E-04*
(iv) z_0 dependent on U, neutral	3.16E-05	2.83E-03	2.43E-04
(v) z_0 dependent on U, marine heat fluxes	3.16E-05	2.86E-03	2.33E-04

*The surface roughness in these cases was selected to be the same as the mean value for case (v)

†The surface roughness in this case was selected to be the same as the mean value for case (iv)

Table 5.4 Predicted values of u_* (m/s)

Scheme	*Minimum*	*Maximum*	*Mean*
(i) Constant z_0, land Bowen ratio	0.008	0.999	0.252
(ii) Constant z_0, land Bowen ratio, neutral	0.025	0.999	0.297
(iii) Constant z_0, marine Bowen ratio	0.008	0.995	0.226
(iv) z_0 dependent on U, neutral	0.023	1.242	0.300
(v) z_0 dependent on U, marine heat fluxes	0.014	1.248	0.288

Table 5.5 Predicted values of sensible heat flux (W/m^2)

Scheme	*Minimum*	*Maximum*	*Mean*
(i) Constant z_0, land Bowen ratio	-84	163	-2
(ii) Constant z_0, land Bowen ratio, neutral	0	0	0
(iii) Constant z_0, marine Bowen ratio	-84	26	-15
(iv) z_0 dependent on U, neutral	0	0	0
(v) z_0 dependent on U, marine heat fluxes	-121	133	2

Table 5.6 Predicted values of latent heat flux (W/m^2)

Scheme	*Minimum*	*Maximum*	*Mean*
(i) Constant z_0, land Bowen ratio	0	293	31
(ii) Constant z_0, land Bowen ratio, neutral	0	0	0
(iii) Constant z_0, marine Bowen ratio	0	424	7
(iv) z_0 dependent on U, neutral	0	0	0
(v) z_0 dependent on U, marine heat fluxes	-198	1114	124

Table 5.3 shows that if a scheme where z_0 depends on the wind speed is selected, then the range of values of z_0 covers about two orders of magnitude. A scatter plot of z_0 against wind speed U calculated using scheme (v) is shown in Figure 5.2. For U greater than a critical value of about 3m/s, z_0 increases with U. Below this value, z_0 increases as U decreases.

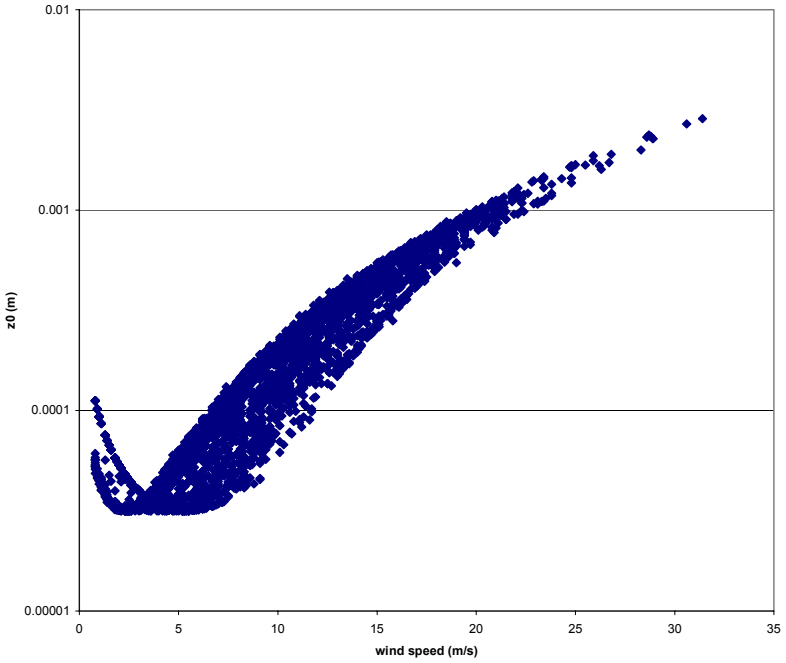

Figure 5.2 Scatter plot of surface roughness against wind speed for scheme (v)

As shown in Table 5.4, using the schemes in which z_0 varies with U tends to increase the value of u_*.

As expected, reducing the Bowen ratio increases the latent heat flux and decreases the sensible heat flux. However, comparison with the results obtained using the marine heat flux algorithms suggests that simply adjusting the Bowen ratio may decrease the sensible heat flux too much, while not increasing the latent heat flux enough. If the marine heat flux algorithms are used, some very large values of latent heat flux are predicted.

When the marine heat flux algorithms are used, the surface sensible heat flux is strongly correlated to the air-sea temperature difference, as shown in the time series plots in Figures 5.3 and 5.4.

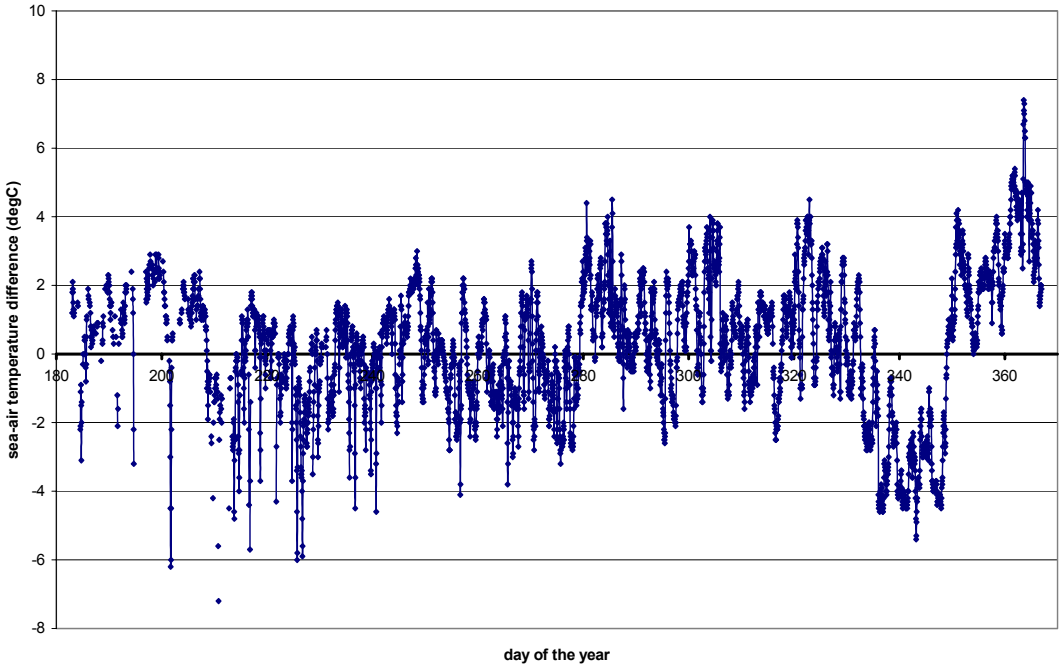

Figure 5.3 Time series of sea surface temperature minus air temperature (°C) at Sean Papa

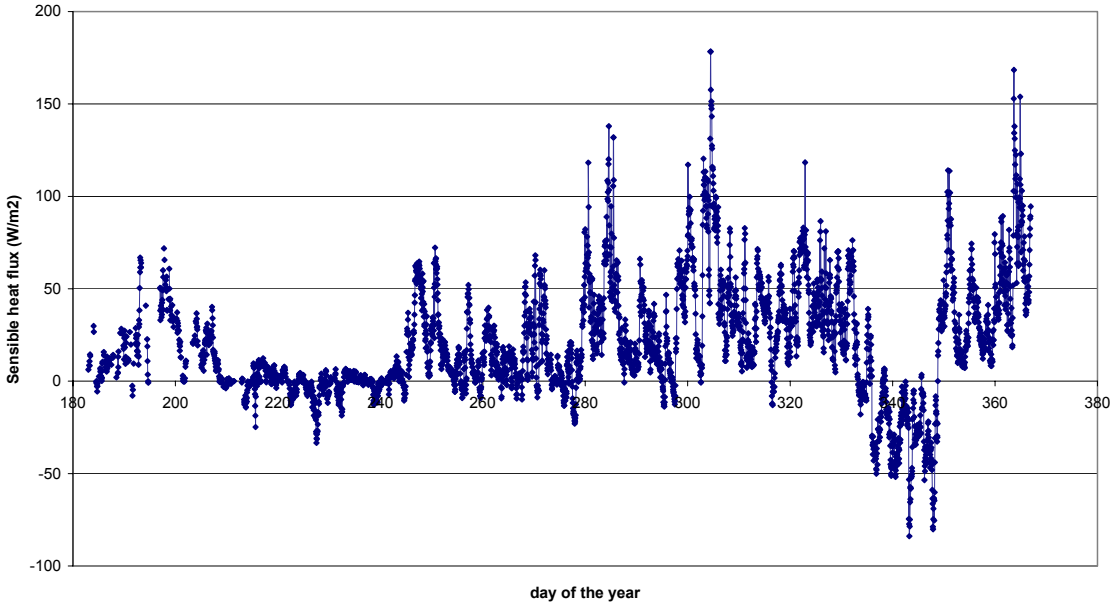

Figure 5.4 Time series of predicted sensible heat flux (W/m^2) at Sean Papa

5.2.4 Effect on dispersion

For each of the sources described in Section 5.2.2, long term mean, maximum hourly mean (100^{th} percentile) and 99.9^{th} and 98^{th} percentile ground level concentrations were calculated using each of the schemes described in Section 5.2.1. The maximum concentrations for each of the sources are summarised in Tables 5.7 to 5.10.

Table 5.7 Maximum concentrations ($\mu g/m^3$) for 5m source, passive release

Scheme	*Long term mean*	*Maximum (100^{th} percentile)*	*99.9^{th} percentile*	*98^{th} percentile*
(ii) Constant z_0, land Bowen ratio, neutral	54.2	2477	2113	734
(iv) z_0 dependent on U, neutral	48.4	2208	1881	628
(i) Constant z_0, land Bowen ratio	43.3	7262	4105	545
(iii) Constant z_0, marine Bowen ratio	39.0	6987	1460	514
(v) z_0 dependent on U, marine heat fluxes	53.2	6876	3719	652

Table 5.8 Maximum concentrations ($\mu g/m^3$) for 30m source, passive release

Scheme	*Long term mean*	*Maximum (100^{th} percentile)*	*99.9^{th} percentile*	*98^{th} percentile*
(ii) Constant z_0, land Bowen ratio, neutral	1.10	45.7	43.6	16.0
(iv) z_0 dependent on U, neutral	1.02	39.3	37.5	14.4
(i) Constant z_0, land Bowen ratio	0.914	254	208	12.5
(iii) Constant z_0, marine Bowen ratio	0.408	255	45.0	6.84
(v) z_0 dependent on U, marine heat fluxes	1.00	238	116	15.2

Table 5.9 Maximum concentrations ($\mu g/m^3$) for 100m source, passive release

Scheme	*Long term mean*	*Maximum (100^{th} percentile)*	*99.9^{th} percentile*	*98^{th} percentile*
(ii) Constant z_0, land Bowen ratio, neutral	0.079	4.48	4.21	1.15
(iv) z_0 dependent on U, neutral	0.070	4.29	3.49	1.02
(i) Constant z_0, land Bowen ratio	0.088	26.7	22.1	1.14
(iii) Constant z_0, marine Bowen ratio	0.017	21.2	4.90	0.306
(v) z_0 dependent on U, marine heat fluxes	0.080	22.6	9.49	1.35

Table 5.10 Maximum concentrations ($\mu g/m^3$) for typical buoyant release

Scheme	*Long term mean*	*Maximum (100^{th} percentile)*	*99.9^{th} percentile*	*98^{th} percentile*
(ii) Constant z_0, land Bowen ratio, neutral	0.102	2.07	2.03	1.58
(iv) z_0 dependent on U, neutral	0.104	2.30	2.27	1.66
(i) Constant z_0, land Bowen ratio	0.099	10.5	7.90	1.81
(iii) Constant z_0, marine Bowen ratio	0.059	2.66	2.15	1.31
(v) z_0 dependent on U, marine heat fluxes	0.111	4.17	3.36	1.85

Looking first at the results obtained assuming neutral conditions (schemes (ii) and (iv)), it can be seen that for the passive releases, using scheme (iv) (allowing z_0 to depend on U) decreases the concentration results. Conversely, for the buoyant release, concentrations increase slightly. This is because, as seen in Section 5.2.3, using scheme (iv) increases u_*, so there is more turbulence, which enhances dispersion, allowing the plume to spread more freely. For the passive releases, which remain relatively close to the ground, increasing the vertical spread has the effect of mixing material upwards, decreasing the ground level concentrations. Conversely, the buoyant release, which rises very quickly, is subject to increased mixing downwards, increasing ground level concentrations. The percentage difference between the results for schemes (ii) and (iv) is typically around 10-15%.

Next consider the effect of using a marine value of the Bowen ratio compared to a land value (schemes (iii) and (i)). As seen in Section 5.2.3, if a marine value is used, the sensible heat flux is reduced. This increases the stability, reducing the vertical mixing and decreasing the ground level concentrations. Concentrations decrease by up to 80%, indicating a strong sensitivity to the choice of Bowen ratio.

Finally, consider the difference between the marine and land heat flux calculations (schemes (v) and (i)). Using the marine algorithms tends to increase the long term mean and low percentile concentrations but reduce the high percentile concentrations. These changes can be explained by reference to the sensible heat flux data in Table 5.5. For this particular meteorological dataset, when the marine flux algorithms are used, the average sensible heat flux is positive, i.e. typically conditions are convective, whereas when the land algorithms are used, the average heat flux is negative, signifying stable conditions. In convective conditions there is more vertical mixing, bringing more of the plume material down to ground level, so concentrations are higher than in stable conditions. Hence the long term mean and low percentiles are higher when the marine flux algorithms are used. (This tendency is probably due to the choice of met. data – because only the second half of the year was used, when typically the sea is warmer than the land, it is to be expected that the marine algorithms would typically predict a positive sensible heat flux.) However, the *maximum* sensible heat flux is lower when the marine flux algorithms are used, hence the maximum concentrations (i.e. the high percentiles) are lower.

5.3 Comparison with observed data

This section describes a comparison of the marine heat flux parameterisation described in Section 5.1(v) with data observed over the Baltic Sea. Section 5.3.1 describes the site and measurements. The results of the comparison are presented in Section 5.3.2. The sensitivity of the results to the Charnock parameter is investigated in Section 5.3.3, and the effect of nearby land is discussed in Section 5.3.4.

5.3.1 Site and measurements

As described in Section 3.2, a study was undertaken by the Danish research institute RISØ in the Baltic Sea over a period of about 10 days in October - November 1998 ([7]). Measurements were made at the small islands of Christiansø, 20km to the north-east of the larger island of Bornholm (Figure 5.5), and about 100km south of the Swedish coast. A measurement mast was set up, on which measurements of sensible heat, latent heat and momentum fluxes were taken at approximately 10m above sea level. RISØ produced 30-minute average values of u_* and heat fluxes from these measurements. (For the purposes of the current study, the 30-minute measurements were averaged to produce hourly average values.) Synoptic measurements of wind (at 10m asl), temperature and humidity were obtained from a lighthouse a few hundred metres from the mast. During the period of the study, two measurements of sea surface temperature in the waters surrounding the islands were taken. For the current study, it has been assumed that the sea was at a constant temperature equal to the average of the two measurements (9.35°C).

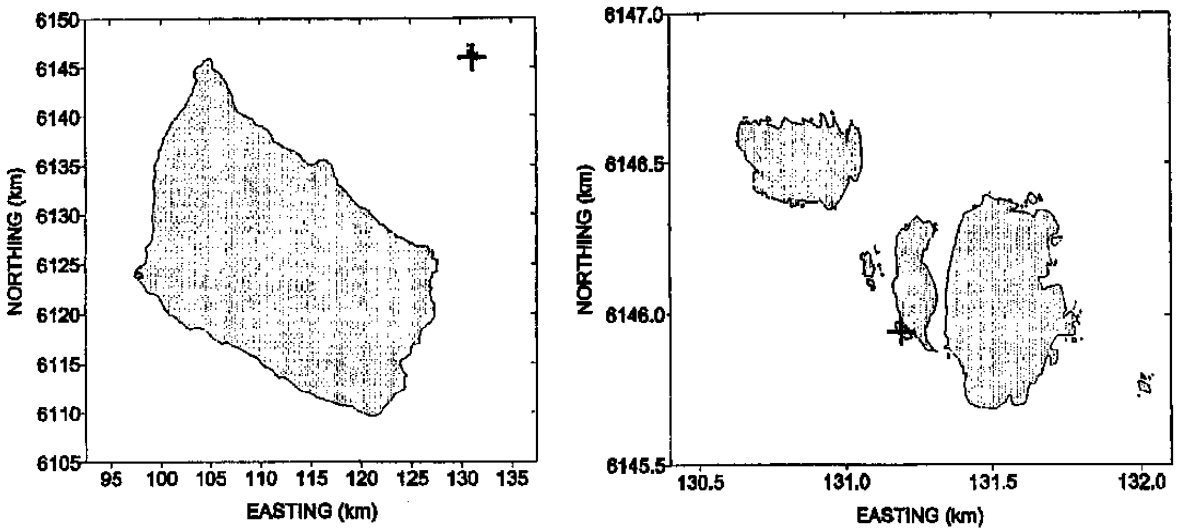

Figure 5.5 Location of measurement site (marked with a cross). The left-hand map shows the island of Bornholm and the location of Christiansø relative to it. The right-hand map shows the islands of Christiansø in greater detail.

Time series graphs of the wind speed and direction are shown in Figures 5.6 and 5.7. For the first three-quarters of the experiment it can be seen that there was a fairly strong wind from the south-west or west, i.e. across the open sea from the direction of Bornholm. In the last

part of the experiment the wind was lighter, and came from northerly and easterly directions, so the immediate fetch was over the islands of Christiansø.

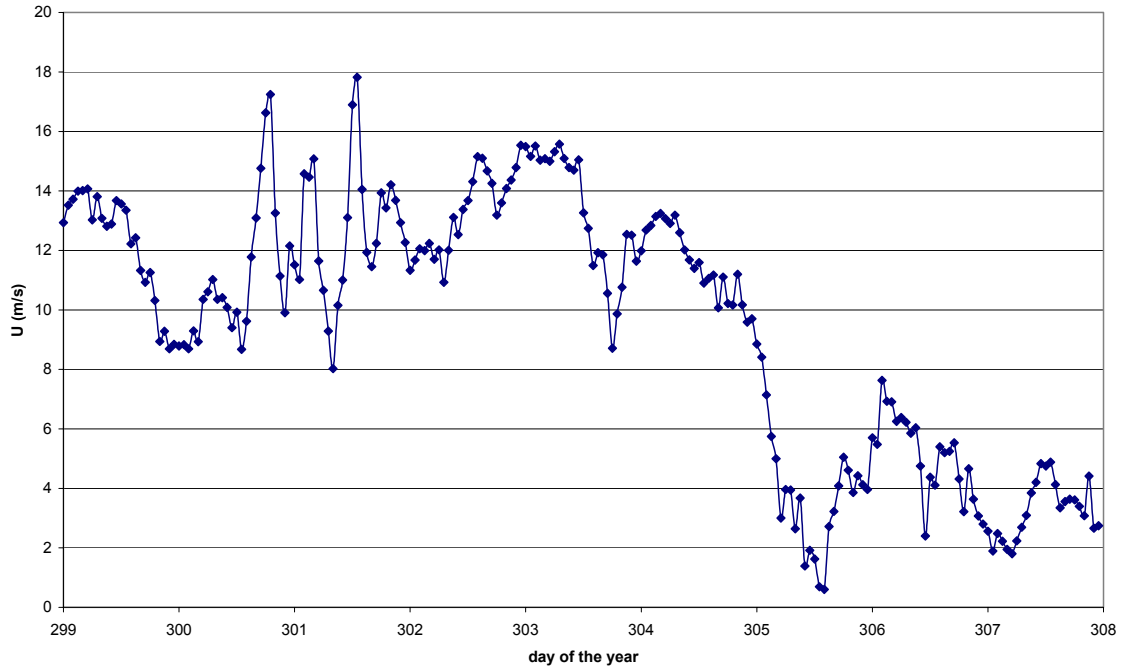

Figure 5.6 Time series of wind speed (m/s) at Christiansø

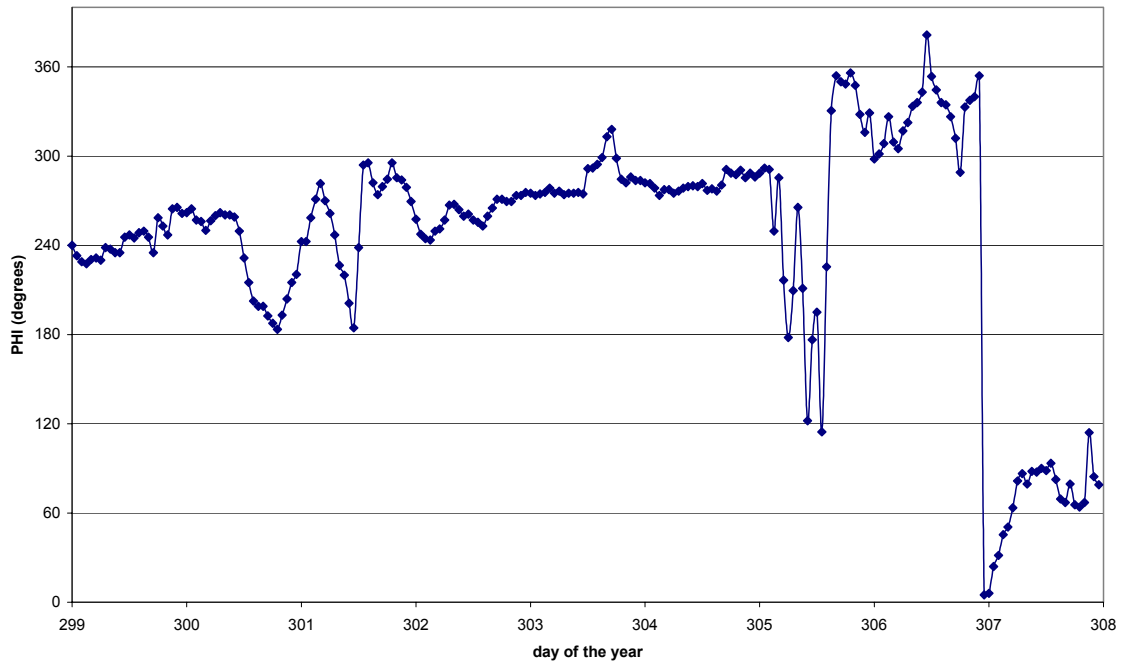

Figure 5.7 Time series of wind direction (degrees) at Christiansø

5.3.2 Comparison of observed and predicted data

Values of u_* and the sensible heat flux were predicted using scheme (v) described in Section 5.1. In this scheme, the surface roughness and friction velocity are assumed to be co-dependent, and heat fluxes are calculated using a scheme suitable for marine use.

A time series plot of the predicted values of surface roughness is shown in Figure 5.8. Comparison with Figure 5.6 shows that the values are closely linked to the wind speed. Typically the value is around 0.0005m during the first part of the experiment, and about an order of magnitude lower during the last part of the experiment.

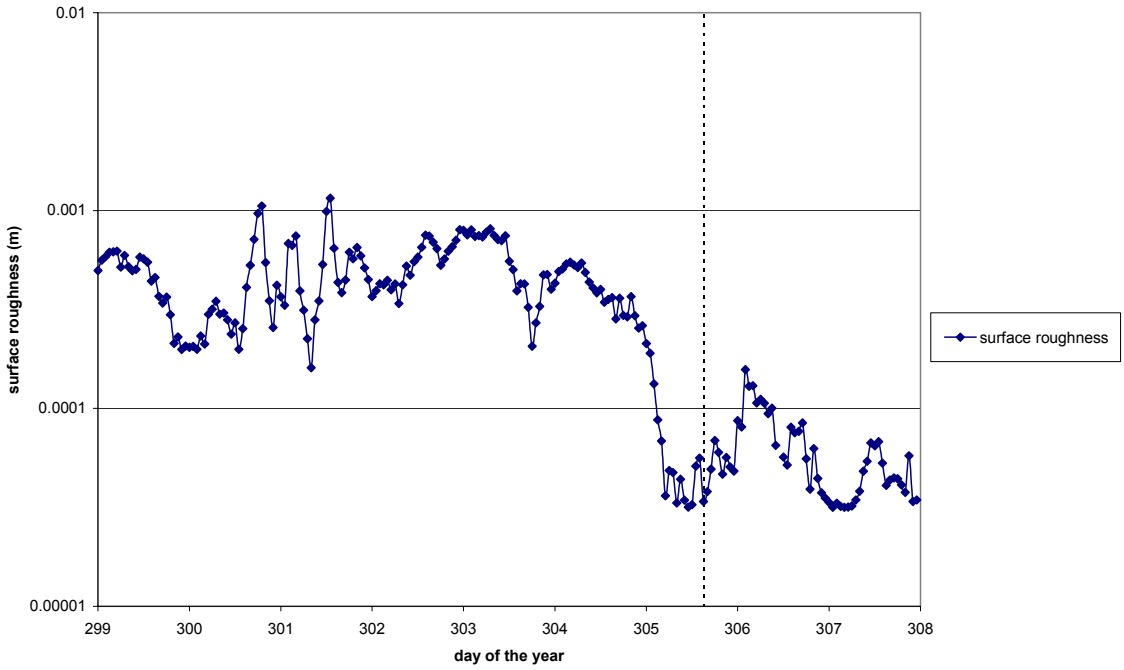

Figure 5.8 Time series of predicted values of surface roughness (m) at Christiansø. The time at which the wind direction switched from south-westerly to northerly/easterly is shown by a dotted line.

Statistics of the observed and predicted values of u_* and the sensible heat flux are presented in Table 5.11. (Since the observed relative humidity data were very sparse, predictions of latent heat flux were not carried out.) These statistics were calculated using data from the first part of the experiment only (i.e. when the immediate fetch was over the sea), as it is not really appropriate to use the marine algorithms when the immediate fetch is over land. Both u_* and the magnitude of the sensible heat flux are somewhat underpredicted. However, the correlation between the observed and predicted values of u_* is very good.

Table 5.11 Observed and predicted values of u_* and sensible heat flux at Christiansø

		Minimum	*Maximum*	*Mean*	*Correlation*
u_* (m/s)	*Observed*	0.059	1.216	0.464	-
	Predicted	0.029	0.793	0.613	0.95
Sensible heat flux (W/m^2)	*Observed*	-46.5	106.8	18.8	-
	Predicted	-25.4	86.2	43.3	0.76

Figure 5.9 shows a time series plot of the observed and predicted values of u_*. Again it can be seen that although the general trends are well predicted (i.e. the correlation is good), the model tends to underestimate, in particular at the peaks. This may suggest that an adjustment to the Charnock parameter α_{Ch} is appropriate in this situation – see Section 5.3.3 below. Also, as the immediate fetch is over land during the last part of the experiment, it is not appropriate to use marine algorithms to calculate u_* during this time. This is discussed further in Section 5.3.4 below.

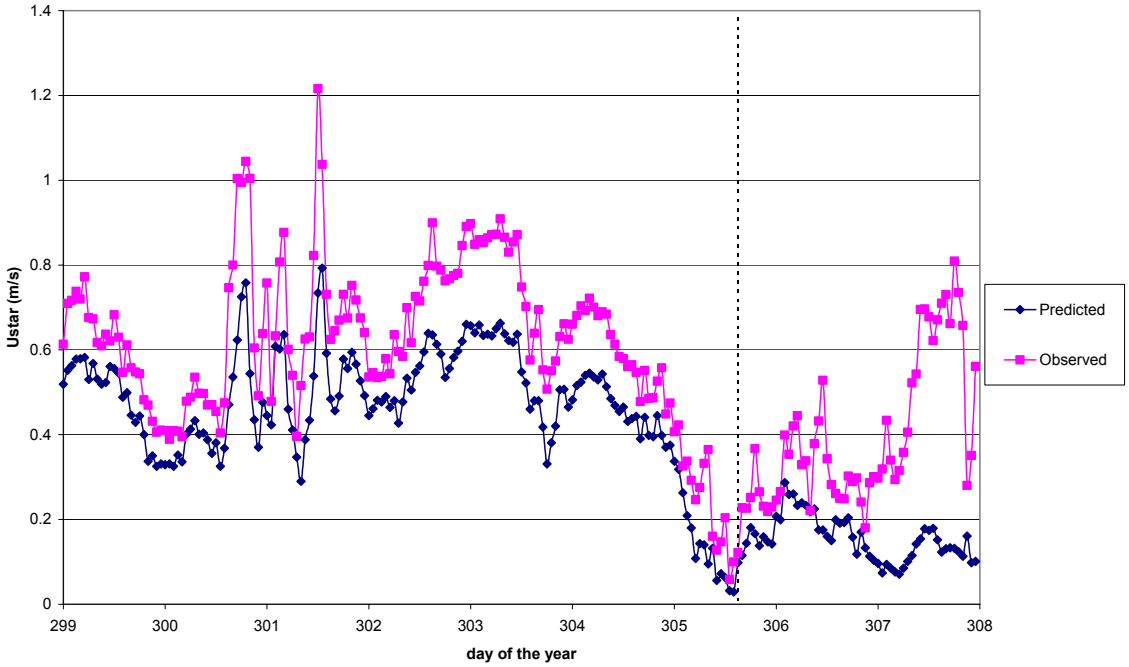

Figure 5.9 Time series of predicted and observed values of u_* (m/s) at Christiansø. The time at which the wind direction switched from south-westerly to northerly/easterly is shown by a dotted line.

A time series plot of the observed and predicted values of sensible heat flux is shown in Figure 5.10. Again the trends are well predicted, although there is some underestimation, particularly during the first part of the experiment when the wind speed is high.

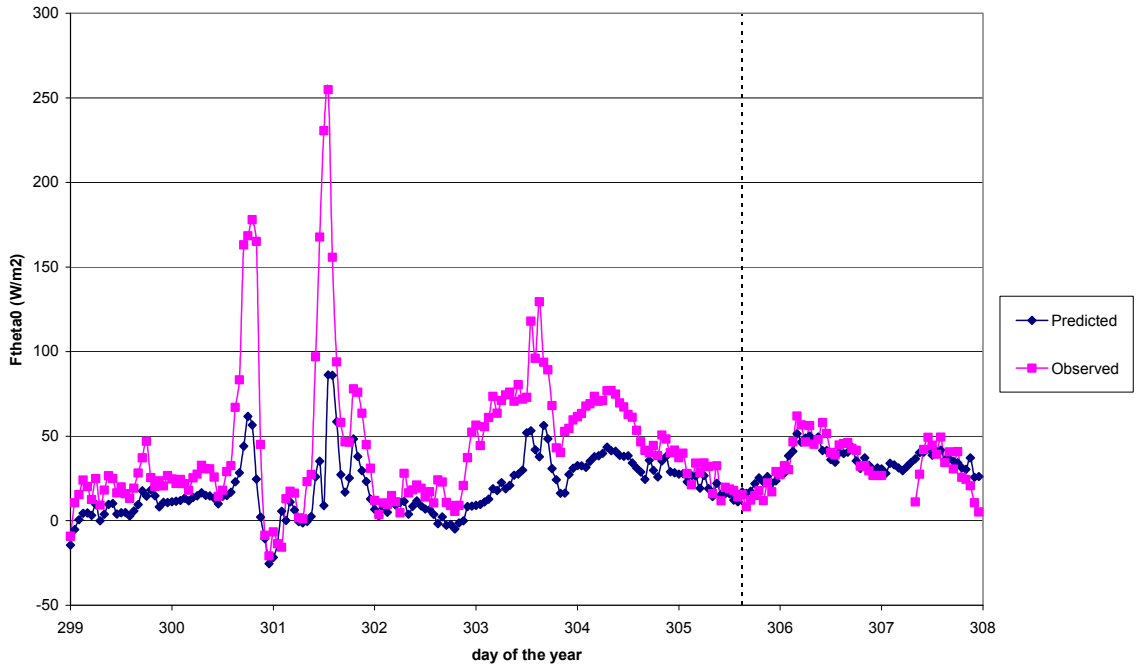

Figure 5.10 Time series of predicted and observed values of sensible heat flux (W/m^2) at Christiansø. The time at which the wind direction switched from south-westerly to northerly/easterly is shown by a dotted line.

5.3.3 Sensitivity of results to Charnock parameter

The effect of changing the value of the Charnock parameter α_{Ch} has been investigated. The results presented in Section 5.3.2 above were produced using α_{Ch} = 0.018. The calculations have been repeated using values of 0.032 (a value commonly used for modelling purposes) and 0.08 (somewhat higher than the range of values recommended by Garratt [1]). The predicted values of u_* (again just for the part of the experiment where the immediate fetch is over the sea) are summarised in Table 5.12. There is no effect on the minimum predicted value of u_*, but the mean and maximum values increase with α_{Ch}.

Table 5.12 Statistics of u_* for various values of Charnock parameter

	Minimum	*Maximum*	*Mean*
Observed	0.059	1.216	0.613
Predicted (α_{Ch} = 0.018)	0.029	0.793	0.464
Predicted (α_{Ch} = 0.032)	0.029	0.863	0.500
Predicted (α_{Ch} = 0.08)	0.029	1.012	0.573

Time series plots are shown in Figure 5.11. The value of α_{Ch} has little effect when the wind speed is low. However, for higher wind speeds, the predictions of u_* improve as α_{Ch}

increases. For $\alpha_{Ch} = 0.08$, there is very good agreement between the observed and predicted values of u_*, when the immediate fetch is over the sea.

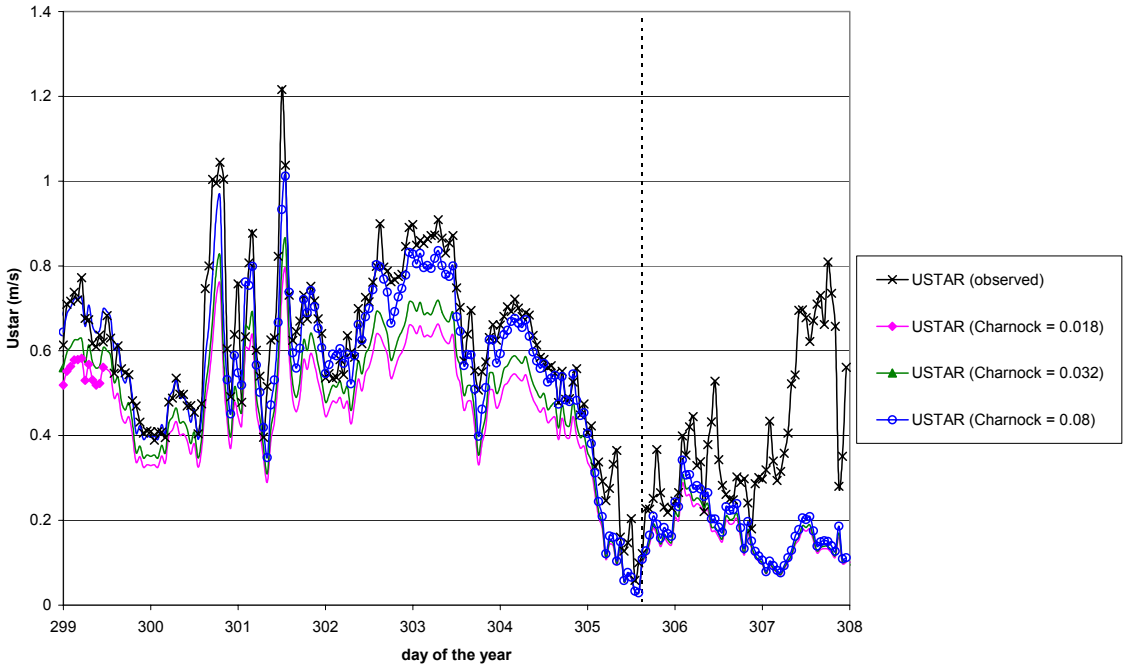

Figure 5.11 Time series of predicted values of u_* (m/s) for various values of α_{Ch}, and observed values, at Christiansø. The time at which the wind direction switched from south-westerly to northerly/easterly is shown by a dotted line.

The value of α_{Ch} was found to have little effect on the predictions of sensible heat flux, although there was a very slight increase with α_{Ch}.

5.3.4 Effect of nearby land

As seen in Figure 5.7, during the experiment the wind was mostly from the south-west, but for the last two days of the experiment the wind moved to a more northerly then an easterly direction. For these later wind directions (in particular for easterly winds) the immediate fetch upwind of the measurement mast is over the islands of Christiansø rather than the sea. The land surface will affect the wind profile, and hence for this part of the experiment it is not appropriate to use a marine algorithm to calculate the surface roughness.

The effect of using a constant surface roughness appropriate for the land during the latter part of the experiment has been investigated. The islands of Christiansø are small and rocky. The island on which the mast is placed is rather flat, but the largest island reaches a maximum height of 20m. Whilst a spatially variable roughness model (for example FLOWSTAR [12]) could be used to investigate the impact of the islands in detail, in the current study an investigation of the impact of the roughness variations was achieved by selecting a range of surface roughness values appropriate for these conditions - calculations were carried out using surface roughness values of 0.01m, 0.1m and 0.3m. Note that all of these values are somewhat higher than those predicted to be appropriate for the sea (Figure 5.8).

The values of u_* predicted using this range of surface roughness values for the latter part of the experiment are shown in Figure 5.12. The observed values, and the values predicted using the marine algorithms, are also included for reference. Up to the start of day 307, the surface roughness value giving predictions of u_* which most closely match the observed values is 0.01m. It is to be expected that a low value of surface roughness would give good agreement here, since during this time, the wind was from the north, so the immediate fetch was over a fairly flat island. During the final day of the experiment, when the immediate fetch was over the largest of the islands, a higher value of surface roughness (0.3m) gives the best agreement with observations.

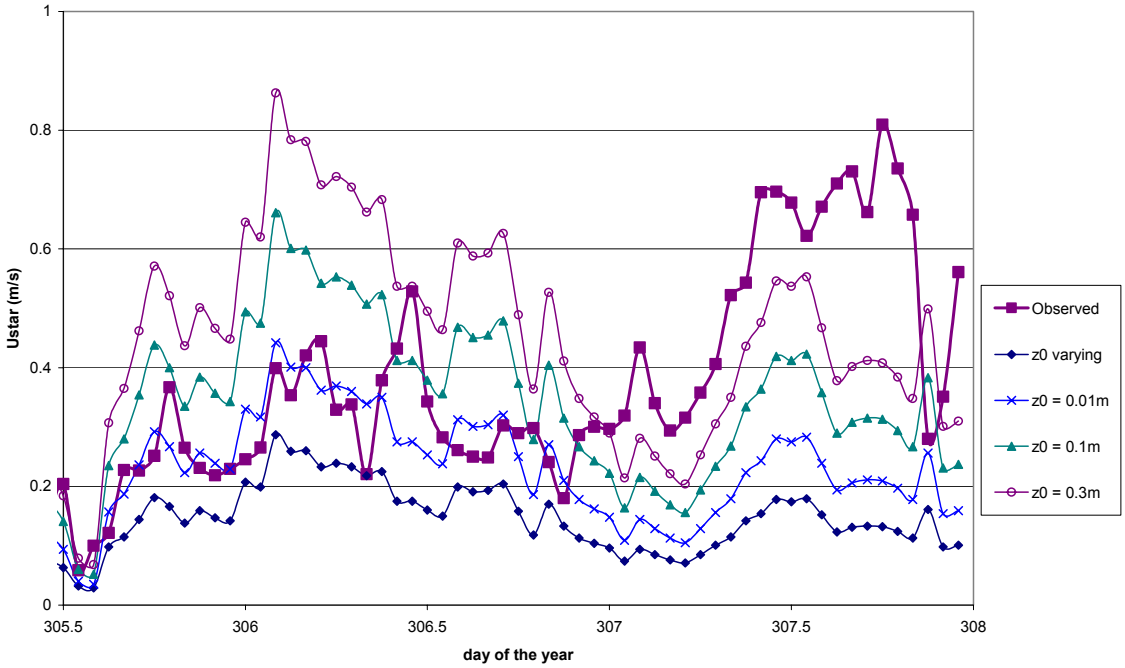

Figure 5.12 Time series of predicted values of u_* (m/s) for various values of surface roughness, and observed values, at Christiansø, during the period when the immediate fetch was over land.

5.4 Further comparison of parameterisations

In Section 5.3.3 it was seen that the best agreement with observed data for a fetch over the sea was obtained using a relatively high value of 0.08 for the Charnock parameter α_{Ch}. It is therefore of interest to revisit the sensitivity study carried out using data from Sean Papa in Section 5.2, to investigate the effect of increasing α_{Ch} on these results.

In this section, predictions of surface roughness and friction velocity at Sean Papa using the parameterisation described in Section 5.1(v) (in which the surface roughness value is calculated from wind data) using two values of α_{Ch} (0.018 and 0.08) are compared. In addition, these predictions are compared to those obtained using the scheme described in Section 5.1(vi), in which the surface roughness value is calculated from wave data.

Statistics of the predicted values of surface roughness z_0 are presented in Table 5.13. Figures 5.13 and 5.14 show scatter plots of the surface roughness values predicted using the wave data parameterisation versus those predicted using the wind data parameterisation, for each value of α_{Ch}.

Table 5.13 Statistics of surface roughness z_0 (m) predicted at Sean Papa using parameterisations (v) (dependence on wind speed) and (vi) (dependence on wave data)

	Minimum	*Maximum*	*Mean*
Scheme (v), $\alpha_{Ch} = 0.018$	3.16E-05	2.86E-03	2.33E-04
Scheme (v), $\alpha_{Ch} = 0.08$	5.19E-05	1.81E-02	1.54E-03
Scheme (vi)	4.00E-07	1.32E-01	7.69E-03

From Table 5.13, it can be seen that the parameterisation using wave data (scheme (vi)) yields a larger range of values than that using wind data. The scatter plots show that when the lower value of α_{Ch} is used, the wind data parameterisation predicts much lower values of z_0 than the wave data parameterisation. However, if α_{Ch} is increased to 0.08, there is much better agreement between the two schemes.

The values of friction velocity u_* are summarised in Table 5.14, and scatter plots comparing the two parameterisations for each value of α_{Ch} are shown in Figures 5.13 and 5.14. Again the two schemes agree best when the higher value of α_{Ch} is used, although the wave data parameterisation tends to predict higher values than the wind data parameterisation.

Table 5.14 Statistics of u_* (m/s) predicted at Sean Papa using parameterisations (v) (dependence on wind speed) and (vi) (dependence on wave data)

	Minimum	*Maximum*	*Mean*
Scheme (v), $\alpha_{Ch} = 0.018$	0.014	1.248	0.288
Scheme (v), $\alpha_{Ch} = 0.08$	0.014	1.488	0.368
Scheme (vi)	0.017	1.739	0.438

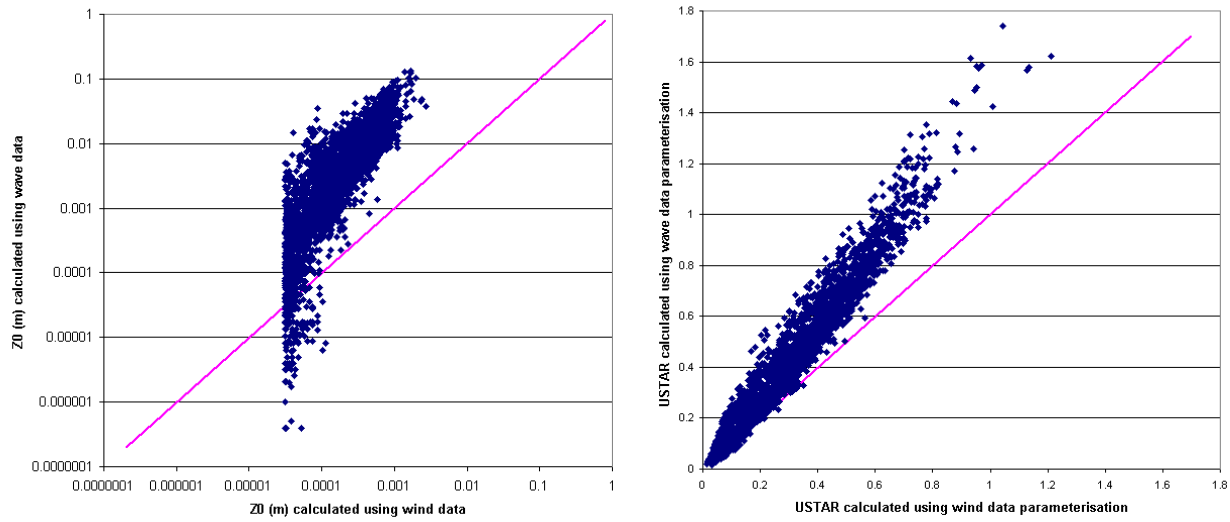

Figure 5.13 Scatter plots of z_0 (m) and u_* (m/s) values predicted using scheme (vi) versus those predicted using scheme (v) with $\alpha_{Ch} = 0.018$

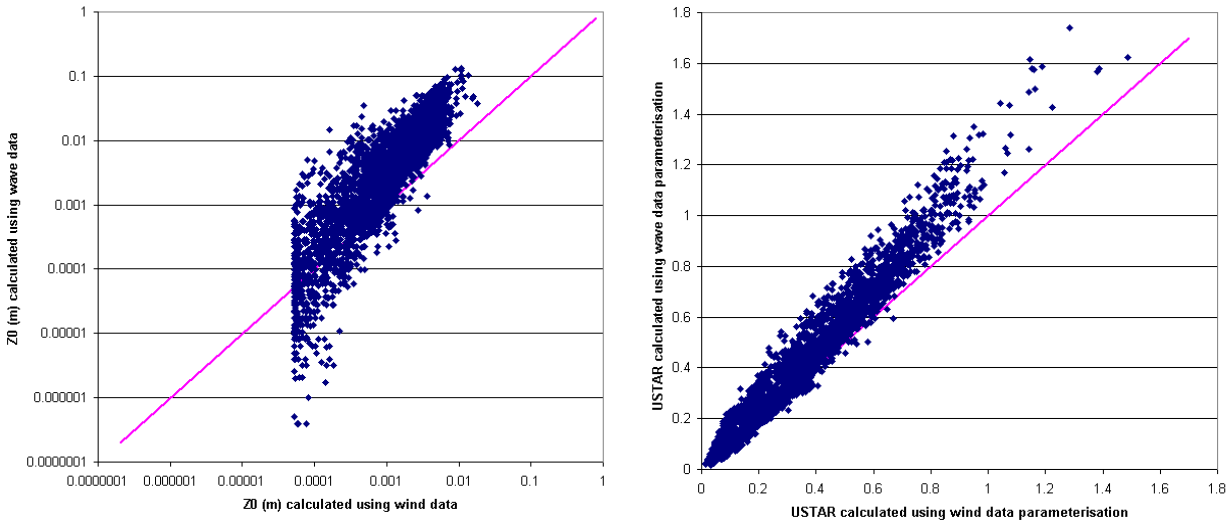

Figure 5.14 Scatter plots of z_0 (m) and u_* (m/s) predicted using scheme (vi) versus those predicted using scheme (v) with $\alpha_{Ch} = 0.08$

6. DISCUSSION AND CONCLUSIONS

In this study,

- sources of offshore meteorological and oceanographic data for the North Sea have been identified;
- current theories of offshore boundary layer structure have been presented; and
- a number of methods of representing the offshore boundary layer in practical dispersion modelling have been presented. These have been compared with each other, and one scheme developed from current theories has been compared with observations.

In this section the results of the study are discussed and some recommendations for practical dispersion modelling of offshore sites are made. Some suggestions for further work are also included.

Standard meteorological data at sites in the North Sea have been found to be available for purchase from a few sources. Although the measurement sites are likely to be more widely spaced over sea than over land, the part of the site-by-site variation observed over the land which is due to local topography will not affect measurements over the open sea. A useful source of sea surface temperature data has also been identified.

Methods of increasing complexity for representing the offshore boundary layer in practical dispersion modelling have been implemented in the dispersion model ADMS. These were tested to investigate their impact on the predicted boundary layer stucture and dispersion, using input meteorological data from the Sean Papa oil platform in the North Sea. It has been shown that allowing the surface roughness to vary with the wind speed tends to increase predicted levels of turbulence and changes ground level concentrations for elevated releases by about 10-15%. The effect of parameterising surface layer heat fluxes over the sea, firstly by simply adjusting the split between the sensible and latent heat fluxes (the Bowen ratio) and secondly by introducing heat flux algorithms appropriate to the marine boundary layer, has been investigated. It was found that the choice of heat flux scheme has a larger difference on dispersion modelling results than the choice of surface roughness parameterisation, changing results for the sources modelled by up to 80%.

The marine heat flux parameterisations rely on the availability of reliable sea surface temperature data in addition to standard meteorological data; however, a good source of sea surface temperature data for the North Sea has been identified in this study. As adjusting the Bowen ratio does not make use of air-sea temperature difference data, this approach could be adopted if sea surface temperature data were not available. However, results suggest that this may not be sufficient to account for the differences in moisture availability and temperature balance over the sea and the land.

Further studies were then conducted using one of the schemes, which included a surface layer heat flux parameterisation and a surface roughness and wind profile parameterisation based on work by Charnock (scheme (v) described in Section 5.1). This was first compared with observed data from the islands of Christiansø, near Bornholm in the Baltic Sea. Trends in u_* and surface heat flux were well predicted, although both were underestimated, suggesting that the predicted values of surface roughness may be

too low. Increasing the Charnock parameter, from commonly used values of 0.018 and 0.032 to 0.08, was found to improve the results. For wind directions when there is land immediately upwind of the site, results were improved by using a constant surface roughness value appropriate for the land.

Support for the higher value of the Charnock parameter of 0.08 was provided by a comparison of surface roughnesses and friction velocities calculated using this scheme with values calculated using a parameterisation based on wave data, using the Sean Papa meteorological data.

Based on the testing of different parameterisations and the comparisons with available data, it is recommended that the following parameterisation of the marine boundary layer is used for atmospheric dispersion modelling for areas which are not altogether remote from land (such as coastal areas and sea areas such as the North Sea, English Channel and Baltic Sea), when the immediate fetch is over the sea:

- Surface roughness and wind profile parameterised using Equation 4.3 (page 9), with a Charnock parameter value of 0.08.

- Surface layer heat fluxes parameterised using Equations 4.7 and 4.11 (page 11).

Note that when using this scheme, the surface roughness (z_0), friction velocity (u_*) and Monin-Obukhov length (L_{MO}) need to be calculated by iteration.

If the site under consideration is directly adjacent to land and the wind is offshore, the usual land-based parameterisation should be utilised.

Whilst the Charnock parameter value of 0.08 is satisfactory for the cases considered in this report, the value is based on limited data and is likely to show significant variation both spatially and temporally.

It is suggested that further work should include obtaining additional observed data with which to compare model results. It is anticipated that the FINO project will be an excellent source of such data in future. Ideally, data should be obtained from a number of sites. Sensitivity to the value of the Charnock parameter α_{Ch} (and the heat flux roughness parameters α_H and α_q) should be investigated so that recommendations for values to use at different types of site (for example coastal, shallow water, open sea) can be made.

7. REFERENCES

[1] Garratt, J.R., 1992: *The atmospheric boundary layer*. Cambridge University Press.

[2] Hinze, J.O., 1975: *Turbulence: An introduction to its mechanism and theory*. 2nd edition, McGraw Hill.

[3] Charnock, H., 1955: *Wind stress on a water surface.* Q. J. R. Meteorol. Soc., 81, 639.

[4] Beljaars, A. C. M., 1994: *The parameterisation of surface fluxes in large-scale models under free convection.* Q. J. R. Meteorol. Soc., 121, 255-270.

[5] Taylor, P.K. and M.J. Yelland, 2001: *The dependence of sea surface roughness on the height and steepness of the waves.* J. Physical Oceanography, 31, 572-590.

[6] Johnson, H.K., J. Hojstrup, H.J.Vested and S.E. Larsen, 1998: *On the dependence of sea surface roughness on wind waves.* J. Physical Oceanography, 28, 1702-1716.

[7] Gryning S.E. and E. Batchvarova, 2002: *Marine boundary layer and turbulent fluxes over the Baltic Sea: measurements and modelling*. Boundary-Layer Meteorol,. 103, 29-47.

[8] CERC, 2001: *ADMS Technical Specification.*

[9] Panofsky, H.A. and J.A. Dutton, 1984: *Atmospheric Turbulence*. Wiley.

[10] US Environmental Protection Agency. *User's Guide for the AERMOD Meteorological Pre-processor (AERMET)*.

[11] Hunt, J.C.R., A. Orr, J.W. Rottman and R. Capon, 2004: *Coriolis effects in mesoscale flows with sharp changes in surface conditions.* Submitted to Q. J. R. Meteorol. Soc.

[12] Carruthers, D.J., J.C.R Hunt and W-S Weng, 1988: *A computational model of stratified turbulent airflow over hills – FLOWSTAR I.* Proceedings of Envirosoft, in Computer Techniques in Environmental Studies, ed. P. Zanetti, 481-492. Springer-Verlag.

[13] Stewart, R.H., 2003: *Introduction to Physical Oceanography*. Open source textbook: http://oceanworld.tamu.edu/resources/ocng_textbook/contents.html

APPENDIX A SUMMARY OF ADMS

ADMS, the Atmospheric Dispersion Modelling System, has been developed to make use of the most up-to-date understanding of the behaviour of the lower levels of the atmosphere in an easy-to-use computer modelling system for atmospheric emissions. This allows the impacts of emissions from industrial and other facilities to be thoroughly investigated as part of an environmental assessment or for other regulatory purposes.

For the current study, ADMS 3 version 3.1.15.0 was used.

The following is a short summary of the capabilities and validation of ADMS 3. More details can be found on the CERC web site at www.cerc.co.uk.

The core model calculates the average concentration arising from an emission for a given meteorological condition (for example, wind speed and direction), taking account of plume rise and stack downwash where required. The emission may be released from a single source or from a number of sources. In addition, ADMS is able to:

- calculate long-term concentration statistics, typically for periods of one or more years, for direct comparison with air quality standards and objectives;
- take into account the often very significant effects that a nearby building can have on the dispersion of emissions;
- model the chemical conversions that occur in the atmosphere between nitric oxide (NO), nitrogen dioxide (NO_2) and ozone (O_3);
- allow for the effects of complex terrain and changes in surface roughness on wind speed and direction, and on the levels of turbulence in the atmosphere;
- determine the quantities of an emission deposited to the ground by both dry and wet deposition processes;
- include the decay of radioactive emissions and determine the gamma dose at a location received from passing material; and
- report the extent to which a moist plume will be visible.

ADMS was developed by CERC in conjunction with the UK Meteorological Office and the Department of Mechanical Engineering at the University of Surrey. In its earlier stages, ADMS was developed with contributions from a number of sponsors, including the Environment Agency (originally under HMIP), the Heath and Safety Executive and a number of the successor companies of the CEGB.

Dispersion Modelling

ADMS uses boundary layer similarity profiles in which the boundary layer structure is characterised by the height of the boundary layer and the Monin-Obukhov length, a length scale dependent on the friction velocity and the heat flux at the ground. This has significant advantages over earlier methods in which the dispersion parameters did not vary with height within the boundary layer.

In stable and neutral conditions, dispersion is represented by a Gaussian distribution. In convective conditions, the vertical distribution takes account of the skewed structure of the vertical component of turbulence. This is necessary to reflect the fact that, under convective conditions, rising air is typically of limited spatial extent but is balanced by descending air extending over a much larger area. This leads to higher ground-level concentrations than would be given by a simple Gaussian representation.

The formulation of ADMS means that, for a given meteorological condition, as well as determining average concentrations the model is also able to provide statistical information on concentration fluctuations. This can be particularly important in applications such as, for example, determining whether or not a dispersing material exceeds flammability or odour detection thresholds.

Emissions

Buoyant emissions, and those with vertical momentum, rise in the atmosphere after emission. This movement, which is referred to as *plume rise*, also results in additional dilution and can result in the emission penetrating the top of the atmospheric boundary layer and being lost from the local area. These effects are included in the modelling using an integral solution of the conservation equations for the plume's mass, momentum and heat.

ADMS can also model emissions represented as:

- lines – for linear sources;
- areas – to represent situations where a source can best be represented as uniformly spread over an area, such as evaporation from an open tank; and
- volumes – to represent situations where a source can best be represented as uniformly spread throughout a volume, such as fugitive emissions from a factory complex.

Presentation of Results

For most situations ADMS is used to model the fate of emissions for a large number of different meteorological conditions. Typically, meteorological data are input for every hour during a year or for a set of conditions representing all those occurring at a given location. ADMS uses these individual results to calculate statistics for the whole data set. These are usually average values, including rolling averages, percentiles and the number of hours for which specified concentration thresholds are exceeded. This allows concentrations to be calculated for direct comparison with air quality standards, guidelines and objectives, in whatever form they are specified.

Results can be presented as numerical values at specified locations. In addition, by calculating concentrations over a grid of locations, results can be presented graphically as concentration contours or isopleths. This is facilitated by a link with the ArcView GIS (Geographical Information System).

Data Comparisons – Model Validation

The individual components of ADMS have been developed using published scientific data and each component extensively tested to ensure that it provides reliable results. In addition, a very large number of studies have been performed on the accuracy of ADMS for point source emissions.

Among other validation studies, ADMS output has been compared with three data sets known as Kincaid, Indianapolis and Prairie Grass, which are readily available from the US Modellers Data Archive. These have been generally accepted as containing enough measurements of sufficient quality for meaningful validation.

Further details of ADMS and model validation, including a full list of references, are available from the CERC web site at www.cerc.co.uk.